RESEARCH

The creep behavior of rock shear seepage under different seepage-water pressures

Guanghe Li[1] · Yanting Wang[1] · Dong Wang[1] · Laigui Wang[1] · Shipeng Zhang[1] · Cunjin Li[2] · Ruixue Teng[2]

Abstract

The long-term compression–shear–seepage coupling of rock mass is a cause of many engineering geological disasters. This study aimed to explore the creep characteristics of rock mass under different seepage conditions. Based on the shear-creep–seepage test results of shale, the shear-creep–seepage model considering damage was constructed using a series connection of the elastomer (H), a nonlinear viscoelastic body with nonlinear function λ (NVEP), a viscoplastic body with seepage switch S (VPB), and a viscoelastic–plastic body considering damage (VEPB). The variation law of the model parameters was analyzed, and the results showed that the model effectively described the entire change process of rock-creep characteristics, notably the deformation law of the accelerated-creep stage. The correlation coefficient R^2 was greater than 0.98, and the fitting curve was highly consistent with the experimental data. Furthermore, the greater the seepage-water pressure, the smaller the shear stress applied in the corresponding test of each stage, and the greater the cumulative shear strain of each stage. Moreover, the seepage-water pressure had a damaging effect on the mechanical strength of the rock samples. The parameter values k_1 and λ were negatively correlated with seepage-water pressure and shear stress, whereas the parameter values k_2 and η_1 were negatively correlated with seepage-water pressure and positively correlated with shear stress. The results of this study can provide theoretical support for the research and analysis of rock-mass engineering stability under long-term seepage conditions.

Keywords Shear–seepage coupling · Injection water pressure · Accelerated phase · Nonlinear model

1 Introduction

Shanxi, Shaanxi, Inner Mongolia, and Ningxia account for 67% of the identified coal reserves in the arid and semiarid regions of Northwest China, which is a large-scale coal-development area in China (Wang 2007). According to the coal-mining practice in the

✉ Y. Wang
  lntu_wyt@163.com

1 College of Mining, Liaoning Technical University, Fuxin 123000, China

2 Inner Mongolia Baiyinhua Mengdong Open-pit Coal Co. Ltd., Xilingol 026000, China

northwest, coal-rich area, the Shanxi–Shaanxi–Inner Mongolia–Ningxia region has abundant underground water despite harboring only 3.9% of the country's water resources (Liu et al. 2019b). Under the action of long-term seepage, the rock in the area easily produces tensile cracks, and the seepage characteristics change, reducing the shear strength of the soil and changing the seepage field (Tang et al. 2011; Liu et al. 2021). The surface and interior of the slope soil form interlaced fracture grids (Long et al. 2019; Zhang et al. 2021), which damage the slope on the surface and internally. Therefore, the creep characteristics of slope rock mass under seepage conditions constitute a scientific problem in the study of slope-instability prevention.

Recently, several authors have studied the influence of seepage on rock-creep characteristics. Wang et al. (2022) established the fractional-order nonlinear perturbation creep model of shale under osmotic pressure. They found that with an increase in osmotic pressure, the fracture mode of shale changed from single brittle fracture to complex brittle and ductile fractures. Through the cyclic loading and unloading test of shale under osmotic pressure, Wang et al. (2021a) found that shale permeability increases with permeability loading and decreases with the unloading of osmotic pressure. Hou et al. (2021) conducted triaxial creep tests of seepage–stress coupling and found that rock-creep deformation increases with increasing seepage-water pressure, and the accelerated-creep stage is attained rapidly. Xia et al. (2020) conducted shear–seepage tests on granite joint samples and observed that the peak shear strength of the joint surface was positively correlated with the normal stiffness, whereas the transmittance and water flow were negatively correlated with the normal stiffness. A seepage evolution model of soft rock was established by Zhou et al. (2020), who studied the influence of seepage on soft-rock damage and failure behavior. The crack-propagation behavior of soft rock under the action of seepage-water pressure was also identified. Li et al. (2020) proposed a macro/micromechanical model for the relationship between creep crack propagation and macroscopic deformation of brittle rock considering the influence of seepage-water pressure. According to the experimental results, the effects of seepage pressure on crack length, crack growth rate, axial strain, and axial strain rate during brittle rock creep were analyzed. Liu et al. (2019a) considered the influence of confining pressure and seepage to establish a nonlinear viscoelastic–plastic creep model under one-dimensional and three-dimensional conditions, providing a basis for creep-deformation prediction under seepage. The Burgers creep model that considers osmotic pressure was developed by Zhao et al. (2019). They analyzed the influence of osmotic pressure on the propagation behavior of decelerating creep crack and steady creep crack of rock, and they verified the rationality of the rock creep-crack model. Xu et al. (2018) proposed a stress–strain constitutive model of rock considering the coupling effect of seepage and stress, and they obtained the complete evolution curve of rock-creep strain under different osmotic pressures as well as the crack-propagation mechanism during rock creep. Shi et al. (2018) found that the shear strength of the joint surface is negatively correlated with the seepage-water pressure but positively correlated with the joint surface roughness and normal pressure.

Evidently, significant progress has been achieved in exploring the mechanism of creep deformation considering seepage and in establishing a corresponding, reasonable creep model. However, only a few studies have investigated the accelerated-creep characteristics and fracture-propagation behavior of weak rock under the influence of seepage. Therefore, the creep characteristics of rock under shear-creep–seepage coupling were investigated in this study using the shear-creep–seepage test results of shale. We established a shear-creep–seepage model considering damage by connecting the following in series: an elastomer (H), a nonlinear viscoelastic body with nonlinear function λ (NVEP), a viscoplastic body with seepage switch S (VPB), and a viscoelastic–plastic body considering damage (VEPB). The

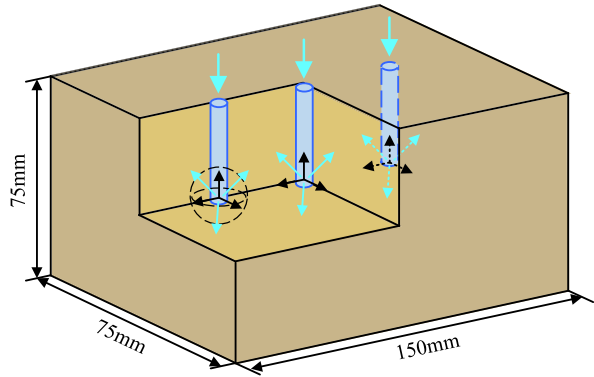**Fig. 1** Schematic of mud-shale sample and water-injection holes

Table 1 Shear-creep–seepage test scheme

Group number	Specimen	Water pressure	Normal load	Duration of water injection per stage load	Shear-loading duration per stage
1	Mud shale	0 MPa	2 MPa	6 h	24 h
2		1 MPa			
3		2 MPa			
4		3 MPa			

results of this study can provide theoretical guidance for researching and analyzing mine slope stability with a weak interlayer.

2 Testing procedures

The rock sample used in the Ma test (Ma et al. 2022a) was mud shale, which was taken from a mining area in Sichuan Province and processed into a cuboid of 150 mm × 75 mm × 75 mm. Three water-injection holes were opened at equal intervals on the upper surface of the rock sample parallel to the center line of the shear direction, as illustrated in Fig. 1. Before the test, the free water-inlet method was used to artificially saturate the rock sample to avoid the influence of changes in water content on the test results during the application of seepage-water pressure. The shear-creep–seepage test was performed on the shale sample, and a normal load of 2 MPa was applied to the rock sample. According to the scheme presented in Table 1, the water-injection holes were injected continuously with water for 6 h at the beginning of each shear loading, and the water injection was stopped when the shear failure of the rock sample occurred. The experimental results are presented in Fig. 2.

3 Analysis of shear-creep–seepage of shale

It can be observed from Fig. 2 that the time–shear-strain curves of shale under different seepage-water pressures had similar trends of four stages (Li et al. 2021): (1) The first stage is the elastic-deformation stage, wherein the rock appears as an elastic body, macroscopically appearing as an instantaneous elastic strain of rock at a high strain rate. (2) The
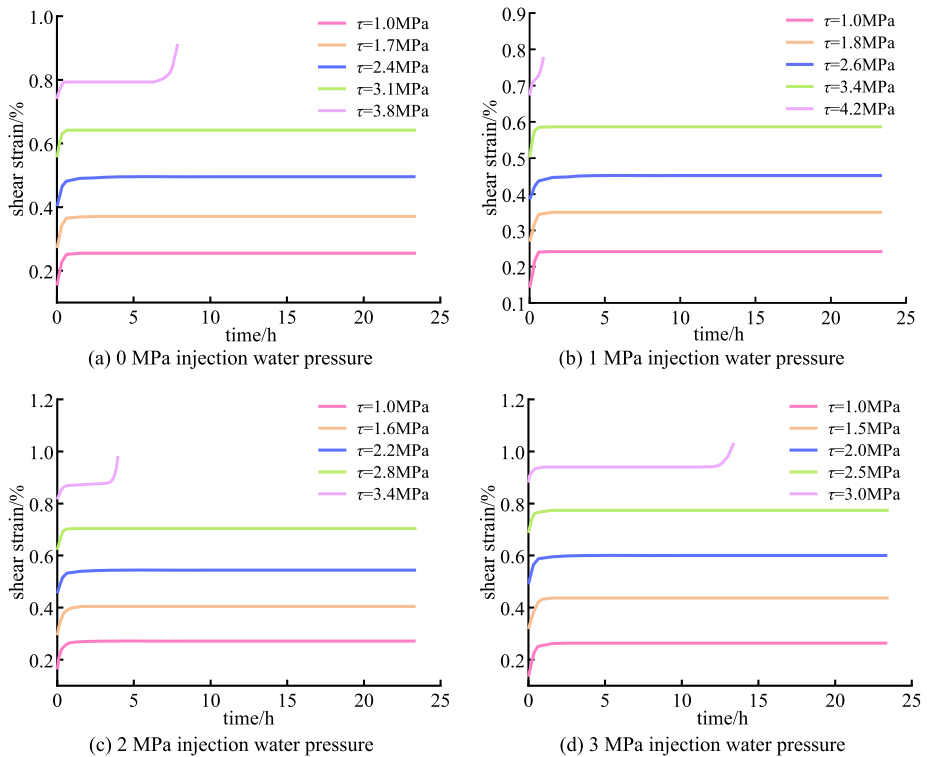
Fig. 2 Shear-creep test curves of shale under different water injection pressures

attenuation-creep stage is the second stage, wherein the primary pores and secondary cracks in the rock gradually close under pressure loading, and the shear deformation of the rock increases slowly with time. (3) In the third stage of constant-velocity deformation, the internal cracks of the rock are closed, the rock deformation rate tends to be stable, and the creep-deformation curve is a straight line. (4) In the final accelerated-deformation stage, because of the increasing shear deformation, the shear cracks caused by irreversible damage start expanding and penetrating. The shear-deformation curve showed a nonlinear change with time and finally resulted in fracture failure. Overall, the rock samples exhibited complex deformation behaviors in the shear-creep tests. Therefore, a reasonable scientific constitutive model is crucial for the accurate description of the creep characteristics and deformation behavior of shale.

4 Shear-creep–seepage model considering damage

The establishment of a constitutive model based on the results of a shear-seepage test is an important part of rock-rheology research. Rocks are generally elastic, viscous, plastic, viscoelastic, and viscoplastic (Li et al. 2023). Thus, it is often difficult for a single-component model to reflect the creep characteristics of rocks fully and accurately. Therefore, according to the basic component criteria, a suitable series–parallel combination is performed to characterize the rheological behavior of rocks (Chen et al. 2021b; Zhao et al. 2022). The

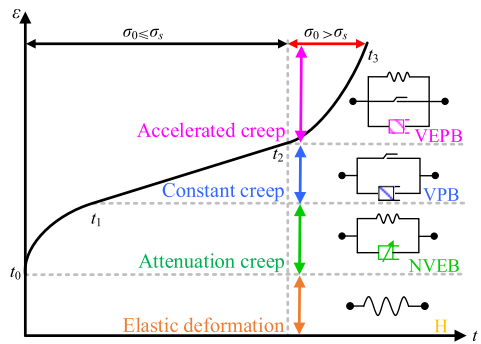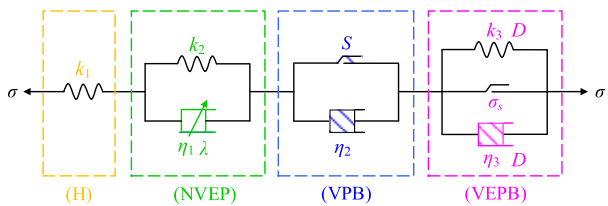**Fig. 3** Rock-creep curve and model-element diagram

Fig. 4 Shear-creep–seepage model considering damage

characterization is based on basic components such as a Hooke elastomer (H), a Newtonian viscous body (N), and a Saint–Venant plastic body (S) (Sun et al. 2021). A creep model is also established to characterize the creep characteristics of shale under seepage.

The elastomer (H), nonlinear viscoelastic body with nonlinear function λ (NVEP), viscoplastic body with seepage switch S (VPB), and viscoelastic–plastic body considering damage (VEPB) are connected in series, and the shear-creep–seepage model considering damage is constructed. The mechanical model and constitutive equation are introduced in Figs. 3 and 4.

At the beginning of the test, the rock specimen produces instantaneous strain, indicating the need for an elastomer in the creep model (Wang et al. 2019). The creep equation of the elastic body is as follows (Wang et al. 2021):

$$\varepsilon_1 = \frac{\sigma}{k_1}, \tag{1}$$

where ε_1 is the strain, %; σ is the stress, MPa; and k_1 is the elastic modulus of the elastomer, MPa.

As the test time increases, the deformation enters the attenuation-creep stage and increases, showing obvious nonlinear characteristics. However, the creep curves of shale differ under different seepage pressures, indicating that the elastic modulus and viscosity coefficient of the model under different seepage pressures are different, and the viscoelastic body should be included in the model. For the viscoelastic body, although the traditional viscoelastic model can better describe the creep-attenuation characteristics under specific stress conditions, the model struggles to reflect the creep nonlinear characteristics effectively under different seepage pressures because of its constant viscous parameters. Therefore, we consider the time correlation of the viscosity coefficient in the viscoelastic body. To establish a nonlinear viscoelastic body, it is assumed that the coefficient satisfies the power-function relationship with time during the creep process. The differential constitutive equation of the

model is as follows:

$$\sigma = k_2 \varepsilon_2 + \eta_1 t^{1-\lambda} \dot{\varepsilon}_2, \tag{2}$$

where ε_2 is the strain, %; σ is the stress, MPa; k_2 is the elastic modulus of the viscoelastic body, MPa; η_1 is the viscosity coefficient of the viscoelastic body, MPa h; and λ is a constant.

The creep equation of the nonlinear viscoelastic body is obtained by solving Eq. (2) (Zhang and Wang 2021):

$$\varepsilon_2 = \frac{\sigma}{k_2} \left[1 - \exp\left(-\frac{k_2}{\eta_1 \lambda} t^\lambda \right) \right]. \tag{3}$$

The viscoplastic body (VPB) with seepage switch S has the following working principle: when the seepage switch is closed, the viscoplastic body works; when the seepage switch is turned on, the viscoplastic body fails. When the seepage switch works, the variation law of the rock in the constant-creep stage is characterized thus: the slope of the creep curve is greater than 0 and increases approximately linearly with time. The creep equation is as follows (Ma et al. 2022b):

$$\varepsilon_3 = \frac{\sigma}{\eta_2} t, \tag{4}$$

where ε_3 is the strain, %; σ is the stress, MPa; and η_2 is the viscosity coefficient of the viscoplastic body, MPa h.

For the viscoelastic–plastic body, the accelerated-creep stage of the rock is characterized. When the rock enters the third stage, internal damage occurs and gradually accumulates, and the rock exhibits obvious nonlinear characteristics (Yang et al. 2022). Therefore, we characterize the creep behavior of rock in the acceleration stage using the viscoelastic–plastic body considering damage.

It is assumed that the damage variable and time of siltstone during creep satisfy a negative exponential function (Zhou et al. 2022; Zhang et al. 2022; Chen et al. 2021a), that is,

$$D = 1 - \exp(-\alpha t), \tag{5}$$

where D is the damage factor, and α is the material constant.

Then, the creep equation is

$$\varepsilon_4 = \frac{\sigma - \sigma_s}{3\eta_3 \exp(-\alpha t)} \left[1 - \exp\left(-\frac{k_3}{\eta_3} t \right) \right], \tag{6}$$

where ε_4 is the strain, %; σ is the stress, MPa; σ_s is yield strength, MPa; k_3 is the elastic modulus of the viscoelastic–plastic body, MPa; and η_3 is the viscosity coefficient of the viscoelastic–plastic body, MPa h.

According to the superposition principle, the elastomer, nonlinear viscoelastic body, viscoplastic body, and viscoelastic–plastic body are connected in series to construct the shear-creep–seepage model considering the damage. When the seepage switch S is opened, the model does not consider the seepage-water pressure, and its creep equation is

$$\begin{aligned} \varepsilon &= \varepsilon_1 + \varepsilon_2 + \varepsilon_4 \\ &= \frac{\sigma}{k_1} + \frac{\sigma}{k_2} \left[1 - \exp\left(-\frac{k_2}{\eta_1 \lambda} t^\lambda \right) \right] + \frac{\sigma - \sigma_s}{3\eta_3 \exp(-\alpha t)} \left[1 - \exp\left(-\frac{k_3}{\eta_3} t \right) \right]. \end{aligned} \tag{7}$$

When the seepage switch S is closed and $\sigma < \sigma_s$, the model considers the seepage-water pressure but not the accelerated-creep stage. The creep equation is

$$\varepsilon = \varepsilon_1 + \varepsilon_2 + \varepsilon_3 = \frac{\sigma}{k_1} + \frac{\sigma}{k_2} \left[1 - \exp\left(-\frac{k_2}{\eta_1 \lambda} t^\lambda \right) \right] + \frac{\sigma}{\eta_2} t. \tag{8}$$

When the seepage switch S is closed and $\sigma > \sigma_s$, the model considers the seepage-water pressure and the accelerated-creep stage. The creep equation is

$$\begin{aligned}
\varepsilon &= \varepsilon_1 + \varepsilon_2 + \varepsilon_3 + \varepsilon_4 \\
&= \frac{\sigma}{k_1} + \frac{\sigma}{k_2} \left[1 - \exp\left(-\frac{k_2}{\eta_1 \lambda} t^\lambda \right) \right] + \frac{\sigma}{\eta_2} t + \frac{\sigma - \sigma_s}{3\eta_3 \exp(-\alpha t)} \left[1 - \exp\left(-\frac{k_3}{\eta_3} t \right) \right].
\end{aligned} \tag{9}$$

Therefore, the creep equation of the shear-creep–seepage model considering damage is as follows:

$$\varepsilon = \begin{cases}
\begin{aligned} &\frac{\sigma}{k_1} + \frac{\sigma}{k_2} \left[1 - \exp\left(-\frac{k_2}{\eta_1 \lambda} t^\lambda \right) \right] \\ &\quad + \frac{\sigma - \sigma_s}{3\eta_3 \exp(-\alpha t)} \left[1 - \exp\left(-\frac{k_3}{\eta_3} t \right) \right], \end{aligned} & S = 0, \\[6pt]
\frac{\sigma}{k_1} + \frac{\sigma}{k_2} \left[1 - \exp\left(-\frac{k_2}{\eta_1 \lambda} t^\lambda \right) \right] + \frac{\sigma}{\eta_2} t, & S > 0, \sigma < \sigma_s, \\[6pt]
\begin{aligned} &\frac{\sigma}{k_1} + \frac{\sigma}{k_2} \left[1 - \exp\left(-\frac{k_2}{\eta_1 \lambda} t^\lambda \right) \right] + \frac{\sigma}{\eta_2} t \\ &\quad + \frac{\sigma - \sigma_s}{3\eta_3 \exp(-\alpha t)} \left[1 - \exp\left(-\frac{k_3}{\eta_3} t \right) \right], \end{aligned} & S > 0, \sigma > \sigma_s.
\end{cases} \tag{10}$$

5 Model validation and parameter identification

To verify the accuracy and effectiveness of the model, fitting analysis was performed on the test results. From the experimental data, ε, σ, and t are known, and the parameters to be determined are k_1, k_2, η_1, λ, η_2, η_3, α, and k_3. Generally, model-parameter determination methods can be divided into graphical methods and optimization analysis algorithms. The optimization analysis algorithm can be divided into the regression analysis and least-squares methods. The least squares method is widely used because it has a high fitting accuracy and combines effectively with numerical software. In this study, the least-squares method was implemented on the mathematical analysis software Matlab to perform nonlinear fitting on the experimental data and to invert the creep parameters. The entire workflow is illustrated in Fig. 5. The parameter-identification results of the shear-creep–seepage model considering damage are presented in Table 2, and the fitting results of the model curve as well as the original data are shown in Fig. 6.

Table 2 and Fig. 6 show that the shear-creep–seepage model considering damage has a better recognition effect and higher fitting accuracy for the creep characteristics of shale under different seepage-water pressures, notably the nonlinear change behavior in the acceleration stage. The fitting curve is highly consistent with the experimental data, and the correlation coefficient R^2 is greater than 0.98. From the description of the creep behavior
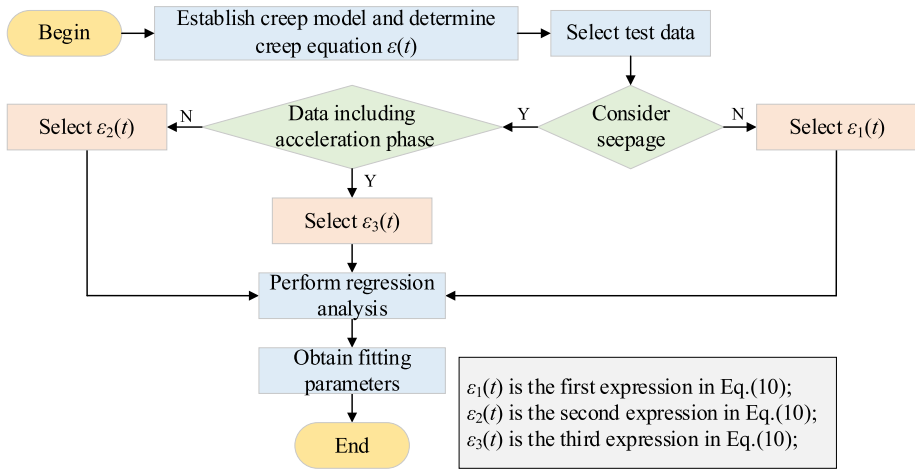
Fig. 5 Workflow diagram

Table 2 Rock-parameter identification results under different seepage-water pressure conditions

| Seepage-water pressure/ MPa	Shear stress/ MPa	k_1 MPa/h	k_2 MPa/h	η_1 MPa/h	λ	η_2 MPa/h	η_3 MPa/h^2	α	k_3 MPa/h	R^2
0	1.0	7.019	10.050	1.634	2.142					0.9999
	1.8	6.701	22.115	3.950	1.715					0.9999
	2.6	6.545	39.691	8.727	1.390					0.9976
	3.4	6.493	54.155	11.064	1.283					0.9998
	4.2	6.246	82.559	13.920	1.062			0.328	2.117	0.704	0.9815
1	1.0	6.519	9.855	0.910	1.610	81891.092				0.9999
	1.7	6.276	17.057	2.856	1.431	57110.024				0.9997
	2.4	5.964	30.258	4.765	1.230	45078.233				0.9963
	3.1	5.577	47.624	6.633	1.142	36570.338				0.9999
	3.8	5.135	71.213	11.790	0.957	30181.985	38564.244	1.509	106.149	0.9828
2	1.0	6.157	9.146	0.760	1.442	56765.715				0.9998
	1.6	5.446	14.411	2.707	1.302	42851.525				0.9998
	2.2	4.843	24.788	3.824	1.152	36706.306				0.9989
	2.8	4.499	38.208	5.360	1.063	27974.966				0.9998
	3.4	4.169	64.673	10.526	0.822	22884.221	14960.382	1.958	2636.656	0.9805
3	1.0	5.847	7.765	0.801	1.323	35359.736				0.9997
	1.5	4.715	12.680	2.808	1.137	22851.593				0.9998
	2.0	4.088	18.187	3.630	1.075	17127.444				0.9987
	2.5	3.642	28.800	4.872	0.955	10852.298				0.9987
	3.0	3.408	50.066	10.265	0.738	8062.872	29209.048	0.995	7.200	0.9962
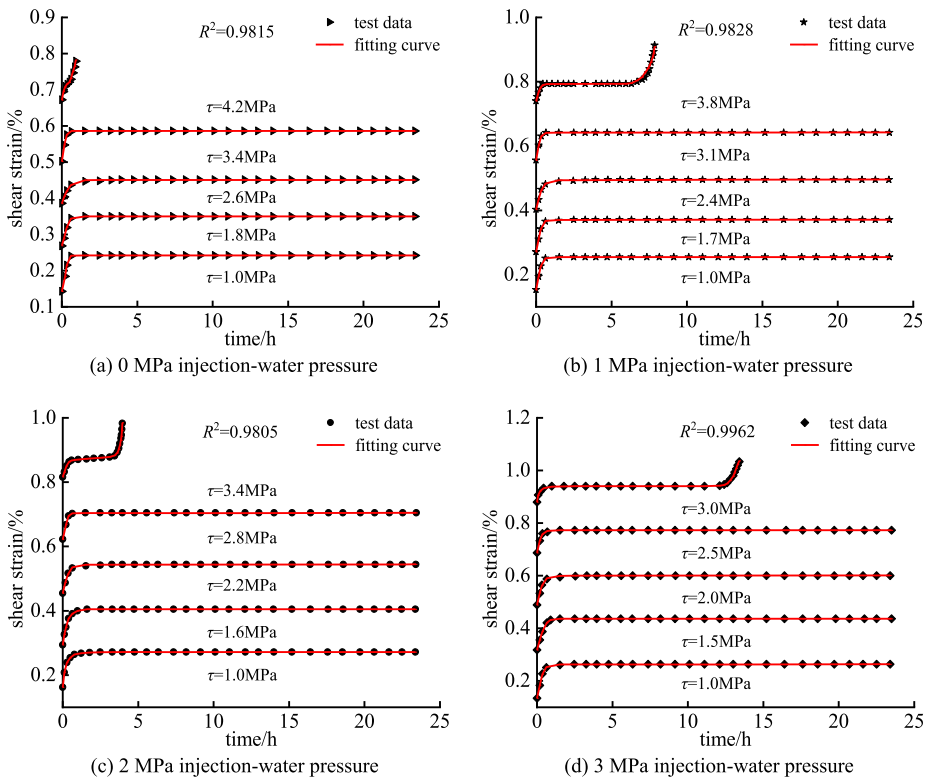
Fig. 6 Fitting-comparison diagrams of test data and theoretical curve under different seepage-water pressures

before and after the acceleration stage, the model is not only suitable for studying the stable-creep-deformation behavior of rock, but also suitable for studying nonlinear accelerated-creep-deformation characteristics. In addition, it can be observed from Figs. 6a–d that under the same normal load, compared with the shear–seepage test results of 0 MPa seepage-water pressure, the failure strength of the rock samples shear creep decreased by 9.52%, 19.05%, and 28.57% when the seepage-water pressure was 1 MPa, 2 MPa, and 3 MPa, respectively. This result shows that the increase in seepage-water pressure is accompanied by a decrease in the shear-creep failure intensity. It can also be seen that under the same shear stress load, the shear deformation of shale follows the seepage pattern. With the increase in permeable pressure, the rock sample saturation increases under the action of permeable water pressure. Thus, seepage-water pressure has a damaging effect on the mechanical strength of rock.

Figure 7 illustrates the cumulative shear-strain curve of shale under different seepage pressures. The analysis shows that the greater the seepage pressure, the smaller the shear stress applied in the corresponding test of each stage, but the greater the cumulative shear strain of each stage. Thus, the larger the seepage-water pressure of the rock sample, the smaller the shear stress required to reach the stable-creep state; the faster the stable-creep stage is attained, the faster the deformation cracks in the rock develop, and the greater the cumulative deformation. The cumulative strain growth of each stage under 3 MPa osmotic water pressure is shown in Table 3 compared with that under 0 MPa, 1 MPa, and 2 MPa osmotic water pressures. The percolation–stress–creep coupling is involved in this process. Changes in the rock osmotic-water pressure change the seepage field and pore-water pres-

Fig. 7 Relationship between shear stress and cumulative shear strain of shale under different seepage-water pressures
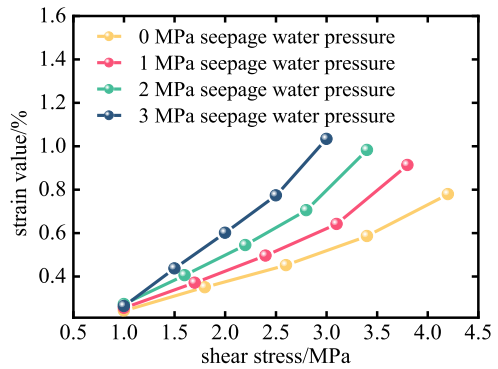

Table 3 Increase in cumulative strain at all levels under other seepage-water pressure conditions relative to 3 MPa seepage-water pressure

Seepage-water pressure	Level 1	Level 2	Level 3	Level 4	Level 5
0 MPa	8.13%	19.85%	24.86%	24.19%	24.59%
1 MPa	3.20%	15.09%	17.50%	17.02%	11.61%
2 MPa	−3.25%	7.23%	9.43%	8.92%	4.87%

Fig. 8 Curve of cumulative seepage-water flow with time under different seepage-water pressures
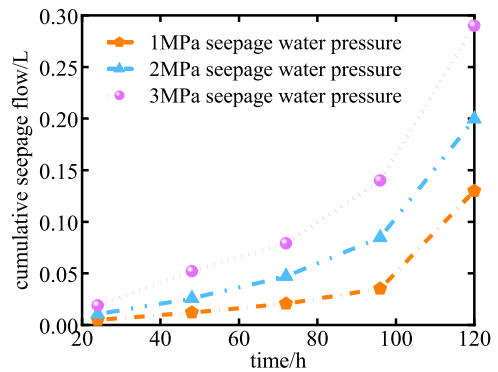
sure, which affects rock deformation and changes the stress field in the rock. Changes in the stress field affect the change in soil-mass stress and strain, which change the permeability coefficient and porosity of the soil mass and finally change the internal seepage field. Then, the seepage field affects the stress field, which is the seepage-stress–creep coupling effect.

Figure 8 shows the curve of cumulative seepage flow with time under different seepage pressures. The greater the seepage pressure, the greater the seepage flow per unit time. According to the preliminary test, as the shear load increases, cracks start forming and developing in the rock sample, which provides a channel for high-pressure water seepage, increasing the water seepage per unit time. An increasing trend is maintained in this process. Before entering the acceleration phase, the seepage rate of 1 MPa, 2 MPa, and 3 MPa is approximately 0.0004 h/L, 0.001 h/L, and 0.0016 h/L, respectively.

At the accelerated-creep stage, the rock sample cracks expand and permeate rapidly, and the high-pressure injected water changes from seepage mainly along the pores and micro-
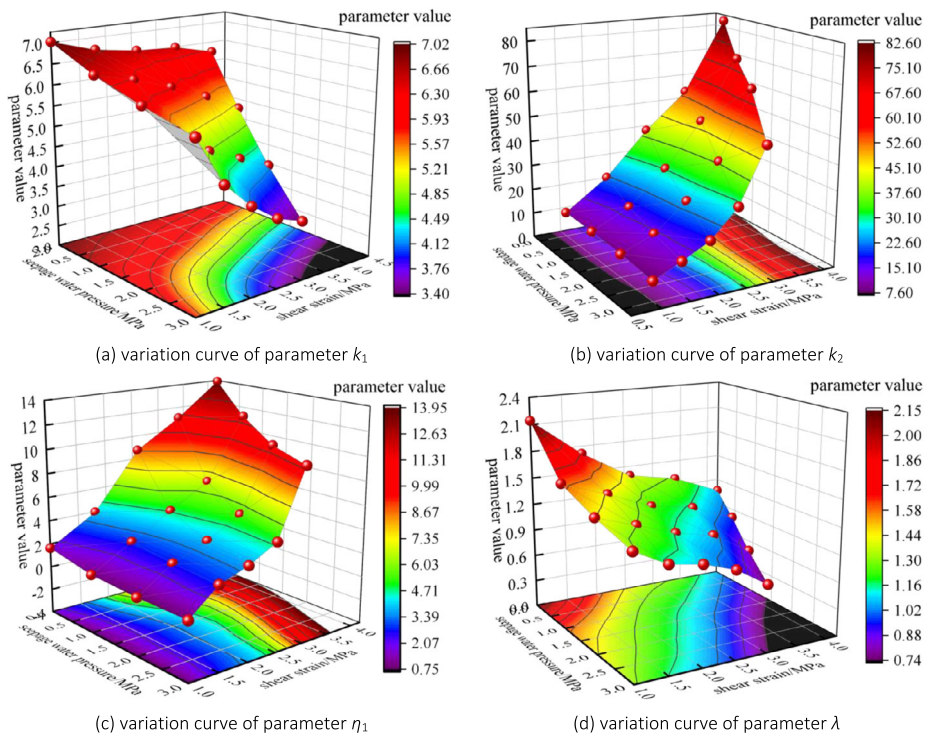
(a) variation curve of parameter k_1

(b) variation curve of parameter k_2

(c) variation curve of parameter η_1

(d) variation curve of parameter λ

Fig. 9 Variation curves of seepage pressure and shear stress with parameter values

cracks to seepage mainly along the penetrating shear cracks. Additionally, the seepage rate and flow rate of the seepage water increase significantly. The seepage rate of 1 MPa, 2 MPa, and 3 MPa is approximately 0.0039 h/L, 0.0048 h/L, and 0.0063 h/L, respectively. This result indicates that the water conductivity of rock samples is closely related to the degree of fracture development. This finding provides important theoretical support for the safe construction and long-term stability analysis of open-pit slope rock mass.

The study of the variation of model parameters is an important part of creep-model research. Because of the different shear stresses of each level corresponding to different seepage-water pressures in this study, we analyzed the model-parameter variation from the perspectives of seepage-water pressure and shear stress. Figure 9 shows a three-dimensional correlation diagram of parameter values against seepage pressure and shear stress. The diagram illustrates the behavior and change trend of the parameter values with two variables: (1) The parameter value k_1 is negatively correlated with both variables, and the slope of the parameter line generated under the same shear stress increases with increasing shear stress. The slope of the parameter line generated under the same level of seepage-water pressure increases with increasing seepage-water pressure. (2) The parameter value k_2 is negatively correlated with the seepage-water pressure and positively correlated with shear stress. The slope o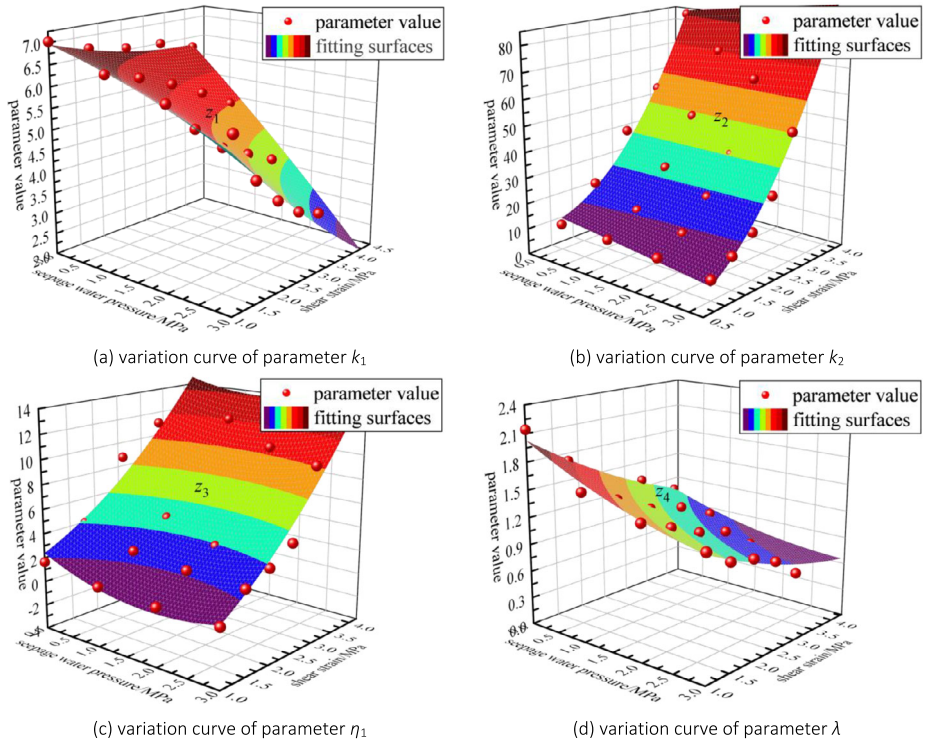f the parameter line generated under the same level of shear stress increases with increasing shear stress. The slope of the parameter line generated under the same level of seepage-water pressure decreases with increasing seepage-water pressure. (3) The parameter value η_1 is negatively correlated with the seepage-water pressure and positively correlated with the shear stress. The slope of the parameter line generated under the same level of shear

(a) variation curve of parameter k_1

(b) variation curve of parameter k_2

(c) variation curve of parameter η_1

(d) variation curve of parameter λ

Fig. 10 Three-dimensional surface-fitting diagram of parameter values

Table 4 Three-dimensional surface-fitting equation and correlation coefficient of parameter values

Parameter	Fitting equation	R^2
k_1	$z_1 = 7.513 - 0.046x - 0.551y - 0.056x^2 + 0.067y^2 - 0.291xy$	0.9828
k_2	$z_2 = 12.750 - 4.096x - 5.411y - 0.034x^2 + 5.332y^2 + 1.723xy$	0.9877
η_1	$z_3 = 0.891 - 2.518x + 0.947y + 0.593x^2 + 0.554y^2 + 0.246xy$	0.9523
λ	$z_4 = 2.461 - 0.394x - 0.423y + 0.039x^2 + 0.032y^2 + 0.035xy$	0.9693

stress increases with increasing shear stress. The slope of the parameter line generated under the same seepage-water pressure only changes slightly, indicating that the shear stress has a greater influence on parameter η_1. (4) The parameter λ is negatively correlated with both variables, and the slope of the parameter line generated from the two angles also decreases as the variables increase. The three-dimensional surface fitting is illustrated in Fig. 10, and the fitting curve is shown in Table 4.

6 Conclusions

(1) Based on the shear-creep–seepage test results of shale, the shear-creep–seepage model considering damage was constructed by connecting the elastomer (H), a nonlinear viscoelastic body with nonlinear function λ (NVEP), a viscoplastic body with seepage

switch S (VPB), and a viscoelastic–plastic body considering creep damage (VEPB) in series.

(2) The model effectively described the entire change process of rock-creep characteristics, notably the deformation behavior of the accelerated-creep stage. The correlation coefficient R^2 was greater than 0.98, and the fitting curve was highly consistent with the experimental data.

(3) The greater the seepage-water pressure, the smaller the shear stress applied in the corresponding test of each stage, and the greater the cumulative shear strain of each stage. Moreover, the seepage-water pressure had a damaging effect on the mechanical strength of the rock samples. The parameter values k_1 and λ were negatively correlated with seepage-water pressure and shear stress. The parameter values k_2 and η_1 were negatively correlated with seepage-water pressure and positively correlated with shear stress.

Availability of data and materials The data used to support the findings of this study are available from the corresponding author upon request.

Code Availability Not applicable.

Declarations

Competing interests The authors declare no competing interests.

References

Chen, W.Z., Lu, C., Yu, H.D., et al.: Progress in long-term mechanical properties of clay rocks under thermo-hydro-mechanical coupling conditions. Chin. J. Rock Mech. Eng. **40**(02), 233–247 (2021b). https://doi.org/10.13722/j.cnki.jrme.2020.0070

Chen, G.Q., Wan, Y., Sun, X., et al.: Research on creep behaviors and fractional order damage model of sandstone subjected to freeze-thaw cycles in different temperature ranges. Chin. J. Rock Mech. Eng. **40**(10), 1962–1975 (2021a). https://doi.org/10.13722/j.cnki.jrme.2021.0064

Hou, J., Guo, Z., Li, J., et al.: Study on triaxial creep test and theoretical model of cemented gangue-fly ash backfill under seepage-stress coupling. Constr. Build. Mater. **273**, 121722 (2021). https://doi.org/10.1016/j.conbuildmat.2020.121722

Li, X.Z., Ban, L.R., Qi, C.Z.: Study on the mechanical model of macro-mecro creep under high seepage pressure in brittle rocks. Rock Soil Mech. **41**(12), 3987–3995 (2020). https://doi.org/10.16285/j.rsm.2020.0453

Li, Z.Y., Yang, G.S., Wei, Y.: Study on creep mechanical properties of frozen Cretaceous sandstone during thawing process. Chin. J. Rock Mech. Eng. **40**(09), 1777–1788 (2021). https://doi.org/10.13722/j.cnki.jrme.2021.0413

Li, X.Z., Jia, Y.X., Yan, H.W., et al.: Mechanism of micro and macro mechanics in brittle rocks during cyclic creep under high seepage pressure. Adv. Eng. Sci., 1–12 [2023-02-13]. https://doi.org/10.15961/j.jsuese.202200431

Liu, X.L., Cao, Z.G., Chen, S.S., et al.: Seepage field analysis and optimal schedule of distributed underground reservoir in mining area. J. China Coal Soc. **44**(12), 3693–3699 (2019b). https://doi.org/10.13225/j.cnki.jccs.SH19.1167

Liu, D., Pu, H., Ju, Y., et al.: A new nonlinear viscoelastic-plastic seepage-creep constitutive model considering the influence of confining pressure. Therm. Sci. **23**, 116 (2019a). https://doi.org/10.2298/TSCI180621116L

Liu, Y., Chen, D.X., Wang, H., et al.: Response analysis of residual soil slope considering crack development under drying-wetting cycles. Rock Soil Mech. **42**(07), 1933–1943+1982 (2021). https://doi.org/10.16285/j.rsm.2020.1504

Long, A.F., Chen, K.S., Ji, Y.X.: Experimental study on wetting-drying cycles of red clay slopes under different rainfall intensities. Chin. J. Geotechn. Eng. **41**(2), 193–196 (2019)

Ma, L.Y., Hu, B., Chen, Y., et al.: Study of shear-seepage properties of intact argillaceous shale under different injection water pressures. Rock Soil Mech. **43**(09), 2515–2524 (2022a). https://doi.org/10.16285/j.rsm.2021.2013

Ma, L.Y., Hu, B., Liu, J., et al.: Study on shear creep damage characteristics of shale block under impact disturbance. Chin. J. Solid Mech. **43**(05), 646–657 (2022b). https://doi.org/10.19636/j.cnki.cjsm42-1250/o3.2022.021

Shi, Z.M., Shen, D.Y., Zhang, Q.Z., et al.: Experimental study on the coupled shear flow behavior of jointed rock samples. Eur. J. Environ. Civ. Eng. **22**, s333–s350 (2018). https://doi.org/10.1080/19648189.2017.1390498

Sun, X.M., Miu, C.Y., Jiang, M., et al.: Experimental and theoretical study on creep behaviors of sandstone with different moisture contents based on modified Nishihara model. Chin. J. Rock Mech. Eng. **40**(12), 2411–2420 (2021). https://doi.org/10.13722/j.cnki.jrme.2021.0302

Tang, C.S., Shi, B., Liu, C., et al.: Experimental characterization of shrinkage and desiccation cracking in thin clay layer. Appl. Clay Sci. **52**(1–2), 69–77 (2011). https://doi.org/10.1016/j.clay.2011.01.032

Wang, Y.G.: The analyse and countermeasures study on the balance of coal market supply and demand in China. Shanxi University of Finance and Economics (2007)

Wang, J.G., Liang, B., Yang, P.J.: Creep experiment and nonlinear disturbance creep model of gneiss under dynamic and static load. J. China Coal Soc. **44**(1), 192–198 (2019). https://doi.org/10.13225/j.cnki.Jccs.2018.5036

Wang, J.G., Sun, Q.G., Liang, B., et al.: Permeability evolution law of shale under cyclic loading and unloading of osmotic pressure. J. Vib. Shock **40**(07), 253–259 (2021a). https://doi.org/10.13465/j.cnki.jvs.2021.07.034

Wang, X.K., Xia, C.C., Zhu, Z.M., et al.: Long-term creep law and constitutive model of extremely soft coal rock subjected to single-stage load. Rock Soil Mech. **42**(08), 2078–2088+2098 (2021). https://doi.org/10.16285/j.rsm.2021.0178

Wang, J.G., Zhang, Q.X., Sun, Q.L., et al.: Macro-meso damage and fracture model for determining the creep characteristics of shale under osmotic pressuresure. J. Mater. Res. Technol. **17**, 2084–2097 (2022). https://doi.org/10.1016/J.JMRT.2022.01.146

Xia, C.C., Yu, Q.F., Qian, X., et al.: Experimental study of shear-seepage behaviour of rock joints under constant normal stiffness. Rock Soil Mech. **41**(01), 57–66+77 (2020). https://doi.org/10.16285/j.rsm.2018.2275

Xu, T., Zhou, G.L., Heap, M.J., et al.: The modeling of time-dependent deformation and fracturing of brittle rocks under varying confining and pore pressures. Rock Mech. Rock Eng. **51**(10), 3241–3263 (2018). https://doi.org/10.1007/s00603-018-1491-4

Yang, C., Xu, X., Wang, L.H., et al.: Relationship between creep characteristics of intact rock and single-flawed sandstone under different critical stress intervals. Chin. J. Rock Mech. Eng. **41**(07), 1347–1357 (2022). https://doi.org/10.13722/j.cnki.jrme.2021.0809

Zhang, L.L., Wang, X.J.: Study on composite creep model of rock considering viscoelastic plastic strain separation. J. Cent. South Univ., Sci. Technol. **52**(5), 1655–1665 (2021). https://doi.org/10.11817/j.issn.1672-7207.2021.05.026

Zhang, Z., Fu, X., Sheng, Q., et al.: Effect of rainfall pattern and crack on the stability of a red bed slope: a case study in Yunnan Province. Adv. Civ. Eng. **2021**(1), Article ID 6658211 (2021)

Zhang, S.L., Liang, W.G., Xiao, N., et al.: A fractional viscoelastic-plastic creep damage model for salt rock considering temperature effect. Chin. J. Rock Mech. Eng. **41**(S2), 3198–3209 (2022). https://doi.org/10.13722/j.cnki.jrme.2021.1237

Zhao, Y., Wang, Y., Wang, W., et al.: Modeling of rheological fracture behavior of rock cracks subjected to hydraulic pressure and far field stresses. Theor. Appl. Fract. Mech. (2019). https://doi.org/10.1016/j.tafmec.2019.01.026

Zhao, L.Y., Lai, Y.M., Niu, F.J., et al.: Multi-scale damage creep model and long-term strength for hard brittle rocks. J. Cent. South Univ., Sci. Technol. **53**(8), 3071–3080 (2022). https://doi.org/10.11817/j.issn.1672-7207.2022.08.024

Zhou, C., Yu, L., You, F., et al.: Coupled seepage and stress model and experiment verification for creep behavior of soft rock. Int. J. Geomech. **20**(9), 04020146 (2020). https://doi.org/10.1061/(ASCE)GM.1943-5622.0001774

Zhou, R.H., Chen, Y., Cai, H.B., et al.: Creep characteristics and creep model of siltstone under triaxial compression and graded unloading. Chin. J. Rock Mech. Eng. **41**(06), 1136–1147 (2022). https://doi.org/10.13722/j.cnki.jrme.2021.1116